JOURNAL OF APPLIED ELECTROCHEMISTRY 24 (1994) 626–631

Electrodiffusion diagnostics of wall shear stresses in impinging jets

S. V. ALEKSEENKO, D. M. MARKOVICH

Institute of Thermophysics, Novosibirsk, Russia

Received 13 May 1993; revised 16 November 1993

The electrodiffusion method of flow diagnostics was applied to the measurement of the wall shear stresses and turbulent characteristics in the vicinity of the stagnation point in impinging jets. The wall shear stress vector was determined by a double electrochemical probe consisting of two electrodes separated by a thin insulation gap. The impingement of an axisymmetric jet on a flat plate at normal incidence and the reattachment of the plane jet to an adjacent solid surface due to the Coanda effect were studied. The influence of injection and suction on the two-dimensional jet reattachment is described.

1. Introduction

The interactions of turbulent jets with solid surfaces occurs in mixing jet chambers, combustors, in the cooling and heating of solid bodies, in jet cleaning of surfaces, and so on. Among the numerous examples of impinging jets the case of a plane jet issuing parallel to a flat plate and reattaching to it due to the Coanda effect is identified [1–3]. Such a flow is shown schematically in Fig. 1. Essentially, the Coanda effect is as follows. The jet issuing along an immediately adjacent plate causes a pressure drop across the jet, which leads to curvature and attachment of the jet to the wall at point x_R.

There are four basic flow regions: (I) the region of the free curved jet, (II) the transition region in the vicinity of the reattachment point (flow with a pressure gradient), (III) the wall jet region, and (IV) the recirculation region. The jet behaviour in region I may be described sufficiently well by integral theories under the assumption that pressure in region IV is constant [2, 3]. In fact the flow structure in the recirculation region is fairly complex and has been little investigated. The laws of wall jet flow in region III are well known.

The neighbourhood of the reattachment point with strongly changing flow parameters is the most difficult for theoretical and experimental study. This zone, however, is of the greatest interest, since the maximum values of heat-transfer coefficients are reached in the vicinity of the stagnation point [4–7]. The wall jets begin to form, moreover, in region II.

The wall shear stress, τ, is an important physical quantity related to heat and mass transfer near the wall. Measurements of averaged values of skin friction for impinging plane jets have been performed by the razor blade technique and heat-transfer probes. An extremely high scatter of the experimental data (up to 100% [7]), due to low precision, is observed both near and away from the stagnation point. The measurements have been made only for impinging jets when the Coanda effect has been negligible. Measurements of the pulsation characteristics of skin friction in plane jets, both impinging and reattaching, are not available in the literature.

The present work is devoted to the study of the wall shear stresses and turbulence characteristics in plane turbulent jet reattachment to the wall (Fig. 1). The investigations were performed under conditions of suction or injection into zone IV in order to exert control over the jet reattachment. The electrodiffusion method for measuring the wall shear stresses was applied allowing detailed investigations in the vicinity of the stagnation point. However, electrochemical probes of small size need careful calibration. In the case of a large experimental set-up the calibration of probes is not easy, since it is difficult to produce a stable flow with known properties [8]. It is easy, however, to create a submerged impinging round jet and this has been studied exten-

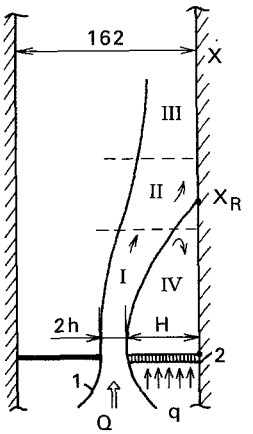

Fig. 1. Schematic view of the test section for studying a reattaching plane jet. (1) Convergent rectangular nozzle and (2) perforated plate.

This paper was presented at the International Workshop on Electrodiffusion Diagnostics of Flows held in Dourdan, France, May 1993.

0021-891X 1994 Chapman & Hall

sively in the literature [4, 5, 9, 10]. Reliable data on skin friction in an impinging circular jet were obtained [9] by an electrodiffusion method. It was shown that the mean wall shear stress in the region of the local maximum is described well by laminar theory based on the momentum equation for flow with a pressure gradient, even at high levels of turbulence. The calibration of skin friction probes, therefore, can be achieved from the calculated maximum shear stress in the vicinity of the stagnation point. However, the neighbourhood of the stagnation point in round impinging jets, as well as in plane jets, has not been adequately studied. Hence, in the present work, additional investigations of the impinging circular jet have been carried out: these are necessary for the improvement of calibration techniques and are connected directly with the case of a plane reattaching jet.

2. Experimental apparatus and instrumentation

The experimental set-up consisted of a test section, two centrifugal pumps, a reservoir, connecting tubes, and apparatus for measurements. The test section was a rectangular vertical channel, made of Plexiglas, and of inner dimensions of 86 mm × 162 mm × 1600 mm (Fig. 1). A plane jet issued from a rectangular convergent nozzle of width $2h$ and length 86 mm. The nozzle length was equal to the channel width since two-dimensional flow resulted. The nozzle unit consisted of separate elements and allowed changing both the nozzle width $2h$ and the nozzle-to-wall distance H.

The plane jet, emerging from the nozzle, curves due to the Coanda effect and attaches to the wall at a point x_R. The Coanda effect may be controlled by the supply (or suction) of liquid with flow rate q into the recirculation zone IV. The ratio q/Q is an injection parameter, where Q is the volumetric flow rate through the main nozzle 1. The experiments were performed for diffusional injection that results from using the perforated plate 2. The hole diameter was 1.5 mm and hole density was approximately 10 cm^{-2}.

Schematic view of the test section for studying an impinging round jet is shown in Fig. 2. The circular convergent nozzle with the exit diameter d was inserted into the channel through the left side wall. An issuing submerged jet impinged normally on the measuring plate 2 that could be shifted along the right wall of the channel upwards and downwards. This plate was also used for the study of a plane reattaching jet. The plate displacement was measured to an accuracy of 0.1 mm. The advantages of using the shifting plate are: one can perform all measurements along the channel axis by the same probe and thus check readings of other probes. This is extremely important for an electrodiffusion method.

The electrodiffusional friction probes were inserted into the measuring plate 2 (Fig. 2(a) and (b)). The sensitive element (electrode) of the probe was a platinum wire (Fig. 2(d)) or sheet (Fig. 2(c)) welded into the glass capillary and ground so as to be flush with the wall surface. The instantaneous wall shear stress was determined by the diffusion current, i, in an electrical circuit of the cathode (probe):

$$\tau = ki^3 \tag{1}$$

where k is the calibration coefficient. The level of shear stress pulsations was calculated by the formula:

$$\tau_0' \equiv (\overline{\tau'^2})^{1/2} = 3k\bar{i}^2(\overline{i'^2})^{1/2} \tag{2}$$

The bar means 'averaging over time', and the prime symbols indicate the pulsation components. Due to the small probe sizes the influence of frequency on the response function was negligible.

The double probe, proposed in [11, 12], is intended for determining friction vector components along the axis O′O″ which is perpendicular to the long side of a probe. If a liquid flows in the direction O′–O″ then the electrode II delivers lower diffusion current than electrode I, because the second electrode is located in the diffusion wake of the first. Thus, comparing the currents of two identical electrodes allows determination of flow direction near the wall.

In the literature there is a limited amount of data, obtained by double electrodiffusion probes. One of the main reasons for this is that it is difficult to manufacture two identical electrodes with very thin spacing (less than 20 μm). Another reason is connected with the complexity of analysing the signals from a double probe when the wall shear stress changes sign.

The electrical scheme of the method is presented in Fig. 3. Each sensitive element of a shear stress probe is

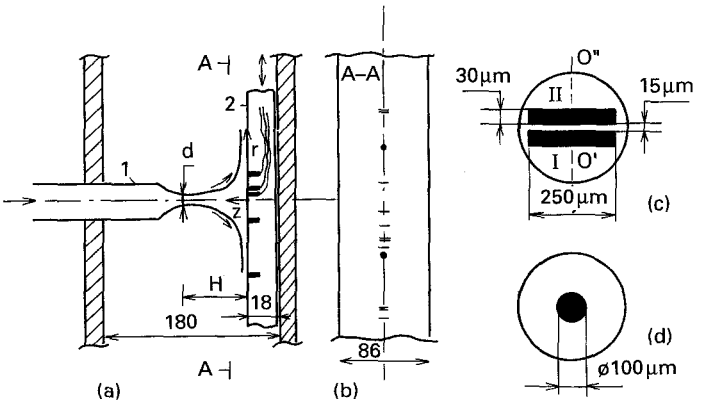

Fig. 2. Schematic view of the test section for studying an impinging circular jet (a, b) and double (c) and single (d) electrodiffusion probes. (1) Convergent circular nozzle and (2) measuring plate.

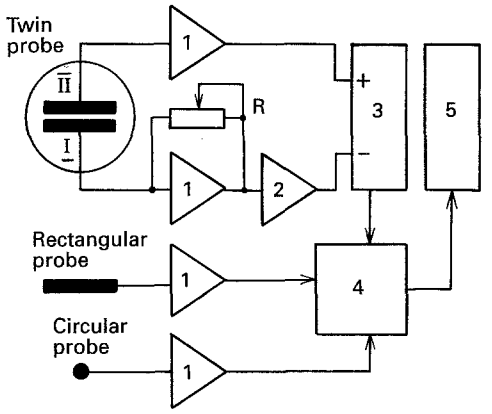

Fig. 3. Electronic scheme of electrodiffusion method. (1) d.c. amplifier, (2) inverter, (3) comparator, (4) multiplexer and (5) computer.

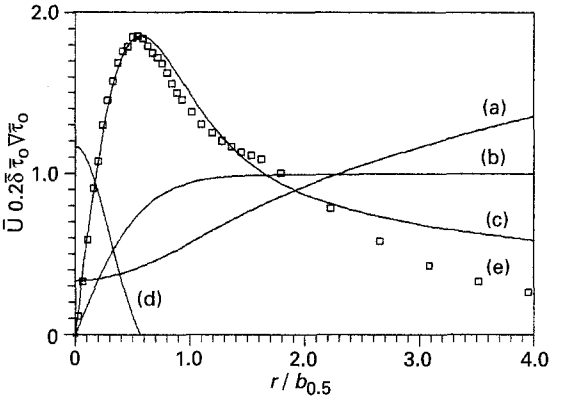

Fig. 4. Radial distributions of wall shear stress, skin friction gradient, boundary-layer thickness and external velocity. Calculations: (a) $0.2\bar{\delta}$, (b) $\bar{U}$, (c) $\bar{\tau}_0$, (d) $\nabla\bar{\tau}_0 = 0.2(\partial\bar{\tau}_0/\partial\bar{r})$, Experiment: (e) $\bar{\tau}_0$ for $\bar{H} = 6$.

connected to a d.c. amplifier with a standard exit signal. In the case of a double probe it is necessary to regulate the gain of the d.c. amplifiers for different electrodes to account for the difference in the probe sizes. The comparison of double probe signals is performed by comparator 3. It is easier to compare the signals of different polarity when an inverter 2 is inserted after one of the amplifiers. The multiplexer 4 is used for commutation of probes. The complete signal processing is accomplished by a computer 5. The technique allows determination of the time of existence of flow with a given direction. All electronic apparatus was developed in the Institute of Thermophysics [13].

The working fluid was an aqueous solution having equimolar concentrations (0.01 M) of potassium ferricyanide and ferrocyanide and a 0.1 M concentration of sodium bicarbonate.

The measuring plate also had 1.0 mm holes as pressure taps. The static pressure was measured by a strain gauge with a sensitivity of 10 mV (mm H_2O)$^{-1}$.

3. Impinging round jet

The flow view is shown in Fig. 2. The single non-dimensional geometrical parameter is a ratio $\bar{H} = H/d$ which changes from 2 to 14. The experiments were performed with a flow with a Reynolds number $Re = V_0 d/\nu = 4.16 \times 10^4$, where $V_0 = 4.33\,\mathrm{m\,s^{-1}}$ is the nozzle exit velocity, $d = 10\,\mathrm{mm}$ is the nozzle diameter, $\nu = 1.04 \times 10^{-6}\,\mathrm{m^2\,s^{-1}}$ is the kinematic viscosity at $T = 22°\,\mathrm{C}$. The turbulence intensity at the nozzle exit, as measured by the electrodiffusion velocimeter [8], did not exceed 1%.

Initially the calibration of the friction probes was made according to the technique described above; that is, the pressure distributions in impinging jet were measured and the maximum shear stress was calculated in the vicinity of stagnation point. As in [9], the pressure distributions in the dimensionless form were similar at $H/d > 6$ and were described by the relation:

$$\bar{P} = 1/(1 + 0.757\,\bar{r}^2)^4 \qquad (3)$$

where $\bar{P} = \Delta P/P_s$, $\bar{r} = r/b_{0.5}$, $b_{0.5}$ is the half-width of the pressure profiles, P_s is the dynamic pressure at the stagnation point. Furthermore, the commonly accepted approach [14] was used for calculating the laminar skin friction in the region with pressure gradient. This is on the basis of the momentum equation with a given distribution of external velocity (or pressure, Equation 3). The results of calculations are presented in Fig. 4. Here $\bar{\tau}_0 = \tau_0\sqrt{(Re_s)}/0.5\rho U_s^2$, $\bar{U} = U/U_s$, U is the external velocity, $U_s = \sqrt{(2P_s/\rho)}$, $\bar{\delta} = \delta\sqrt{(Re_s)}/b_{0.5}$, δ is the boundary-layer thickness, $Re_s = U_s \cdot b_{0.5}/\nu$. The open circles correspond to experimental data for $H - 6$. The probe calibration was completed at the point of maximum friction. The same value of calibration factor k in Equation 1 was obtained for $\bar{H} = 2$, where the turbulence intensity was less than 10%. In this case, however, it was necessary to use an appropriate pressure distribution, but not a self-similar profile (Equation 3).

There is no point in using the experimental data at $\bar{H} > 8$ for calibration of probes because, due to the strong turbulence in the vicinity of the stagnation point, the skin friction values may differ from the theoretically predicted ones.

Figure 5 shows the distributions of an averaged wall shear stress, τ_0, and the relative level of pulsations $(\overline{\tau'^2})^{1/2}/\tau_0^m$ along the radial coordinate, r, for two directions: $\theta = 0°$ (vertically upward, see Fig. 2) and $\theta = 180°$ (vertically downward). The r.m.s. of pulsations are divided by the maximum value of

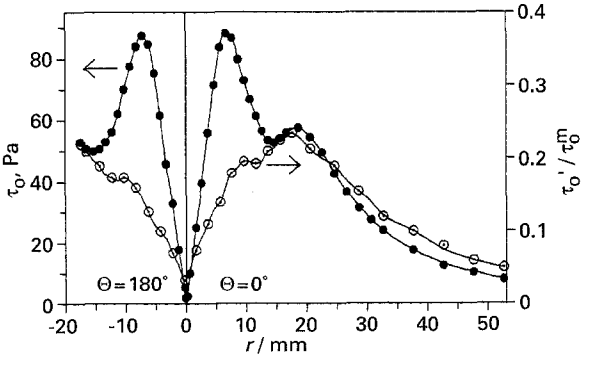

Fig. 5. Distribution of mean skin friction τ_0 and turbulence intensity in the impinging round jet when $H/d = 4$, $Re = 4.16 \times 10^4$.

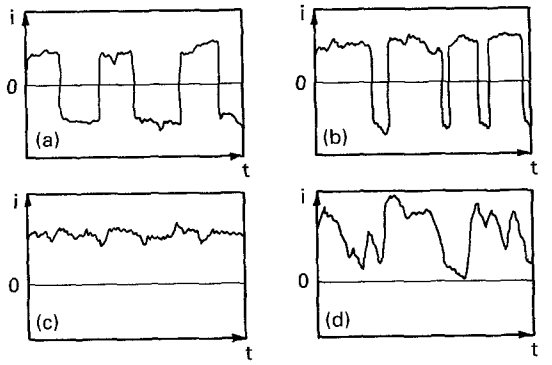

Fig. 6. Oscillograms of diffusion current for double probe against distance from the stagnation point. (a) $r = 0$, (b) $r = 0.3$ mm, (c) $r = 1$ mm and (d) $r = 15$ mm.

skin friction τ_0^m. With the twin probe it is possible to obtain the experimental data directly in the vicinity of the stagnation point. The characteristic oscillograms of diffusion current versus the coordinate r are presented in Fig. 6. In the neighbourhood of the stagnation point the sign of the shear stress varies with time, and the electronic apparatus processes the particular electrode of the twin probe which is the upstream one. The data, presented in Fig. 5, are averaged over the time period taking into consideration a skin friction sign. The transition between direct and back flow occurs abruptly according to the oscillograms *a* and *b* in Fig. 6 as was observed in other works [12, 13] when studying separated flows. To understand such probe behaviour it is necessary to fulfil the special investigations of the pulsating flows with zero mean skin friction.

Turning to the experimental data in Fig. 5, the free jet at $\bar{H} = 4$ still has an initial region in the vicinity of the jet axis and hence the turbulence intensity at the stagnation point is extremely low. The flow is laminar here. The mean shear stress at the stagnation point is zero (previously it was impossible to obtain this result by other experimental methods). With increasing r the wall shear stress grows linearly. At some distance from the stagnation point the local maximum is achieved and then a decrease in shear stress occurs. The wall boundary layer remains laminar, though the pulsations grow progressively. At fairly large distances the boundary layer becomes turbulent, however, and, as a result, the second local maximum of skin friction appears at $r = 18.5$ mm. After the second maximum, both mean shear stress and relative level of pulsations decrease monotonically with distance r. The similar behaviour of curves is observed at all $\bar{H} < 6$ when the initial region exists in a free jet (Fig. 7).

At $\bar{H} > 6$ the jet impinging on a wall has a high level of turbulence since the transition to the fully developed turbulent boundary layer occurs gradually, and the second maximum of mean shear stress does not appear (Fig. 7).

It follows from the experiment that the difficulties of studying the impingement region are connected with the small sizes of this zone and the existence of

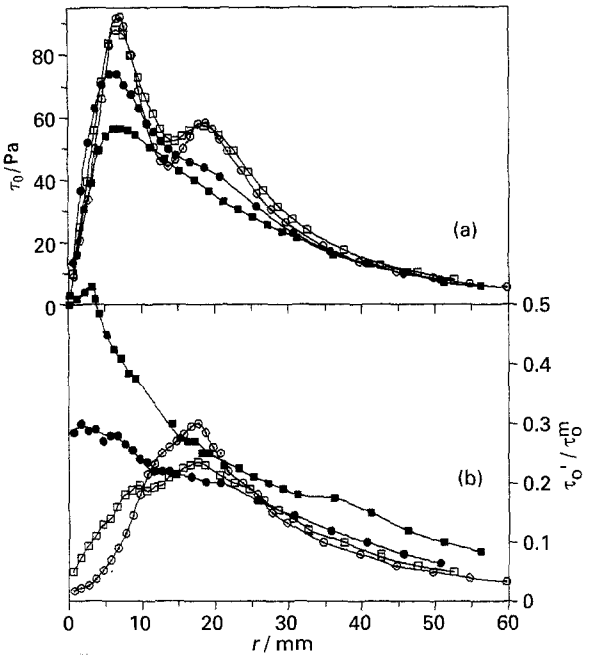

Fig. 7. Distributions of wall shear stress (a) and its turbulence intensity (b) in impinging round jet against the nozzle-to-wall distance $\bar{H} = H/d$, $Re = 4.16 \times 10^4$. H/d: (⊙) 2, (□) 4, (●) 6 and (■) 8.

unsteady back flows which may be characterized by the back flow factor:

$$\gamma = t_-/t_+$$

Here t_-, t_+ are the time intervals over which the back and direct streams near the wall exist. The experimental values of γ against the nozzle-to-wall distance $\bar{H}$ are presented in Fig. 8. All curves have the characteristic shape with a sharp peak in the centre and a smooth change at large r.

The width of the region with unsteady back flows depends strongly on the parameter $\bar{H}$. The absolute dimensions of this zone are very small and change from about one to several millimeters. Outside this region the factor $\gamma = 0$, but at $r \approx 45$ mm ($\bar{H} = 2 \div 8$) and $r \approx 32$ mm ($\bar{H} = 2$; 4) the narrow zones are found where again the back flows appear. They are connected, apparently, with the local separation of boundary layer previously discovered in [10, 15–17] on the basis of visual methods. It is supposed [10, 16] that the local separation is

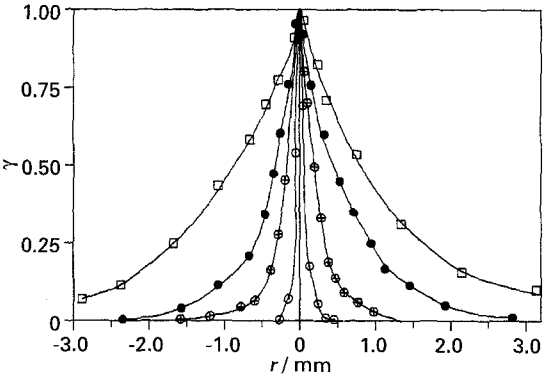

Fig. 8. Back flow factor in impinging round jets. H/d: (⊙) 2, (⊗) 5, (●) 6 and (□) 8.

governed by large-scale vortices (coherent structures) in the external mixing layer which induce local pressure gradients inside the boundary layer.

As noted above, the neighbourhood of stagnation point is of the greatest interest because the maximal values of heat-mass transfer coefficients occur there. It follows from boundary-layer theory that the heat flux at the stagnation point is proportional to the gradient of external velocity dU/dr. For this reason much attention is given in the literature on impinging jets to analysis of this quantity. The main way of determination of the velocity gradient is to use the expression:

$$\left.\frac{dU}{dr}\right|_{r=0} = \left(\frac{1}{\rho}\left.\frac{d^2P}{dr^2}\right|_{r=0}\right)^{1/2}$$

which follows from the momentum equations [4]. Evidently operation of double differentiating on the empirical pressure profile yields essential errors. At the same time from the integral equations one can obtain the relation

$$\left.\frac{dU}{dr}\right|_{r=0} \sim \left.\frac{d\tau_0}{dr}\right|_{r=0}$$

Since there is no problem in determining (with high accuracy) (from Fig. 7) the skin friction gradient at the stagnation point, this method is suitable for analysing the heat-mass transfer processes at the stagnation point.

On the other hand, the gradient of wall shear stress at $\bar{H} < 6$, when the turbulence intensity at the stagnation point is extremely low, would also be appropriate for use in calibration of probes by comparison with laminar theory (Fig. 4).

4. Reattachment of a plane jet to the wall

The flow view at reattachment of a plane jet to the wall due to the Coanda effect is shown in Fig. 1. The main difference of a reattaching jet from the angled impinging jet consists of the existence of a pressure drop across the jet. In this connection there are some peculiarities of flow in the vicinity of the reattachment point x_R. Figure 9 shows the empirical distributions of mean skin friction τ_0 (a), static pressure ΔP (b) and level of shear stress pulsations (c) against the injection factor q/Q at $H/2h = 6$. Here $Re = V_0 \cdot 2h/\nu$, where V_0 is the nozzle exit velocity. The dependencies of τ_0 have a characteristic shape for impinging jets as well as the case when a free jet is fully developed. For this reason every curve has one maximum both to the right and to the left of the stagnation point. The pressure maximum does not correspond exactly to the stagnation point but is displaced downstream. The static pressure in the recirculation zone is negative and varies non-monotonically which points to the complex vortex structure of the zone.

Injection into the recirculation zone ($q/Q > 0$) leads to displacement of the reattachment point

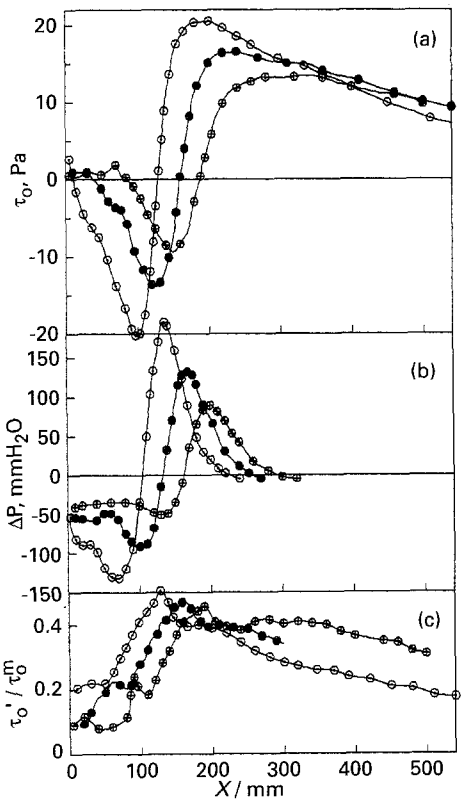

Fig. 9. Distribution of mean shear stress (a), static pressure (b) and turbulence intensity (c) in plane reattaching jet against the injection factor q/Q, $H/2h = 6$, $2h = 12$ mm, $Re = 4.65 \times 10^4$. q/Q: (●) 0, (⊙) −0.15 and (⊗) +0.15.

downstream and to a decrease in the absolute values of skin friction and pressure extremums. Suction yields the opposite effect. These results correspond qualitatively to the theoretical predictions [1, 3].

The maximum values of turbulence intensity are observed in the vicinity of a reattachment point and they depend weakly on the injection and suction (Fig. 9(c)).

The back flow factor, γ, is shown in Fig. 10. It follows from plots that the behaviour of γ in the vicinity of the stagnation point (curves I) is similar to the case of an impinging circular jet. The distribution of γ, moreover, remains symmetrical in spite of the evident asymmetry of the flow. New regions of unsteady back flows (curves II) appear, which are caused by the formation of vortices in the recirculation zone and the interaction of opposite streams at $q/Q > 0$.

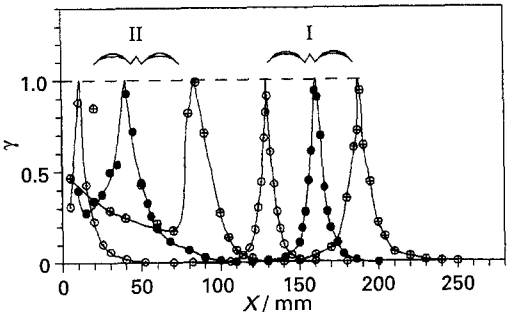

Fig. 10. Back flow factor in plane reattaching jet. q/Q: (●) 0, (⊗) +0.15 and (⊙) −0.15.

The main peculiarity of the presented results is that the absolute values of maximum and minimum mean skin friction are of the same order, though the jet attaches to the wall at a large angle and divides into two distinct wall jets. Thus the commonly accepted assumption [2, 3] of the recirculation zone as a stagnant one is invalid, and needs correction on the basis of the experimental data.

References

[1] S. V. Alekseenko and D. M. Markovich, 'Separated Flows and Jets'. IUTAM Symp., Novosibirsk, USSR, 1990. Springer-Verlag, Berlin, Heidelberg (1991) p. 843.

[2] R. A. Sawyer, *J. Fluid Mech.* **9** (1960) 543.

[3] S. V. Alekseenko, *Sibirski Fiz.-Tekn. Zurnal* **1** (1991) 62, in Russian.

[4] C. DuP. Donaldson and R. S. Snedekar, *J. Fluid Mech.* **45** (1971) 281.

[5] C. DuP. Donaldson, R. S. Snedekar and D. P. Margolis, *ibid.* **45** (1971) 477.

[6] B. N. Yudaev, M. S. Mikhailov and V. K. Savin, 'Heat Transfer at Interaction of Jets with Barriers', Mashinostrojenje, Moscow (1977), in Russian.

[7] E. P. Dyban and A. I. Mazur, 'Convective Heat Transfer at Jet Blowing Bodies', Naukova Dumka, Kiev (1982), in Russian.

[8] S. V. Alekseenko and D. M. Markovich, *Elektrokhimia* **29** (1993) 17, in Russian.

[9] K. Kataoka and T. Mizushina, 5th International Heat Transfer Conference, Tokho (1974) p. 305.

[10] I. B. Ozdemir and J. H. Whitelaw, *J. Fluid Mech.* **240** (1992) 503.

[11] B. Py, *Int. J. Heat Mass Transfer* **16** (1973) 129.

[12] T. J. Hanratty and J. A. Campbell, 'Fluid Mech. Measurements', Hemisphere, Washington (1973) p. 559.

[13] V. E. Nakoryakov, A. P. Burdukov, O. N. Kashinsky and P. I. Geshev, 'Electrodiffusion Method of Studying the Local Structure of Turbulent Flows', Inst. of Thermophysics, Novosibirsk (1986), in Russian.

[14] H. Schlichting, 'Boundary Layer Theory', McGraw-Hill, New York (1960).

[15] J. K. Harvey and F. J. Perry, *AIAA J.* **9** (1971) 1659.

[16] N. Didden and C. M. Ho, *J. Fluid Mech.* **160** (1985) 235.

[17] C. C. Landreth and R. J. Adrian, *Exp. Fluids* **9** (1990) 74.